Gravitational Waves from Fallback Accretion and Black Hole Formation in Long GRBs

K. Gill[1] and S. E. Gossan[2]

[1]*Embry Riddle University, 3700 Willow Creek Road, Prescott Arizona, 86301, USA*
[2]*California Institute of Technology, Pasadena, CA 91125, USA*

We aim to put quantitative constraints on the fraction of long gamma-ray bursts (LGRBs) associated with broad-line type Ic SNe from observations of gravitational waves (GWs). By analyzing the waveforms from Ott et al. (2011) [1], the Piro & Thrane 12 (PT12) analytical model [2], we introduce a new set of phenomenological waveforms for BH formation and different types of stellar collapse. Through the investigation of the detectability of GWs from several emission mechanisms connected to neutron stars, super-luminous supernovae (SLSNe) and LGRBs in the context of Advanced LIGO and Advanced Virgo, in addition to proposed third-generation ground-based GW detectors, such as Einstein Telescope and LIGO Voyager, we propose a radio search focusing entirely on type Ic-BL SNe in low metallicity environments in order to determine a 90% chance of detecting an off-axis LGRB event.

I. INTRODUCTION

A core-collapse supernova (CCSN) that may leave a neutron star (NS) behind, but in the cases where this does not happen, a stellar-mass black hole (BH) is expected instead and can occur in a number of different ways. For example, if there is a nuclear phase transition during protoneutron star (PNS) cooling, or if cooling reduces pressure support in a hypermassive PNS, a BH results. But, if the SN mechanism fails to revive the accretion shock, the continued accretion then pushes the PNS over its maximum mass, which then creates a BH with likely little to no electromagnetic signal [3]. There have been a wide range of predictions for the type of events associated with fallback accretion leading to BHs. However, this work primarily focuses on the case where newly formed BH continues to accrete, produces a jet that may result in a jet-powered Type II SNe or a long gamma-ray burst (LGRB) that may also be pointed away from the observer (or jet formation does not occur at all), and dim supernova could result instead [4–6].

The currently favored delayed explosion mechanism focuses on the explosions in massive stars from the neutron energy deposition exterior to a contracting proto-neutron star [7]. Massive stars ($M \geq 25\ M_{\odot}$) may not always produce a successful explosion via the mechanism described above, but the collapsar model puts forth the failure of the neutrino energy deposition in order to explode the core of massive rotating stars that follow the continued evolution after the stellar core collapses to produce black hole formation and therefore accrete the surrounding stellar mantle [8]. Collapsars generally possess powerful explosions that tap into a fraction of the binding energy released by the accreting star through magnetohydrodynamical processes, neutrino annihilation, or even through the extraction of some of the black hole spin energy [9].

Assuming the fallback material forms a disk before reaching the neutron star, the neutron star accretes sufficient angular momentum that the spin of the neutron star is parameterized through $\beta = T/|W|$ as it reaches a critical value, β_c. T is defined to be the rotational energy and W is the gravitational binding energy. Above β_c, non-axisymmetric instabilities occur and GWs are radiated. Since the NS is quickly torqued down when $\beta > \beta_c$, and spun up by accretion when $\beta < \beta_c$, the NS is then forced into a state of marginal instability when $\beta = \beta_c$ while mass is continuously gained. The high rotation that is required to centrifugally support a disk that is capable of powering a GRB, should produce GWs via bar or fragmentation instabilities that develop in the collapsing core or in the disk above a critical β. Asymmetrically in falling matter is expected to perturb the final BH geometry, ther33eby leading to a ring-down phase. This results in roughly 30 - 3000s of high frequency of GW production until the NS becomes sufficiently massive to follow a collapse into a BH.

Rotation is critically important since the collapsar model involves highly collimated jets produced along the polar axes, arising from a dense, equatorial accretion disc feeding the central black hole. The stellar winds from WR stars hinder the direct measurement of rotational velocities, but polarimetry favors negligible deviation from spherical symmetry in most solar metallicity WR stars. A high angular momentum within the Wolf-Rayet core in the collapsar model [10]. Evolutionary models allowing for magnetic fields involve cores that are efficiently spun down before collapsing, in most models, either due to the shear between the slowly rotating RSG envelope and core, or loss of angular momentum during the WR phase as a result of its high mass-loss rate. These permit the observed rotational rates [8] of young pulsars (e.g. a period of 33 ms for the Crab pulsar) to be reproduced. However, collapsars would require an order of magnitude shorter periods of ≤ 2 ms.

Within the past few years a direct connection has been established between certain type Ic-BL SNe and GRBs, supporting the collapsar model in which the GRB results from the death throes of a rapidly rotating carbon-oxygen (Wolf-Rayet) star. In more distant GRBs, although the afterglow is normally observed, the supernovae are intrin-

sically much fainter and hence are often undetected. The collapsar model involves a compact, rotating hydrogen-deficient massive progenitor, i.e. Wolf-Rayet star. The collapsar model predicts that every LGRB is accompanied by an exploding star, and therefore some of these stellar explosions should be observable as SNe behind the glare of the fading optical counterpart of the GRB [11]. The key components for a successful LGRB/SN are a compact progenitor with a short light-crossing time of roughly 1 s and fast rotation at the time of collapse. One is the collapsar model, a fast-rotating progenitor fails to explode in its early post-bounce phase and instead forms a black hole, while the in-falling envelope eventually forms a Keplerian disk feeding the hole on an accretion/viscous time scale comparable to that of the LGRB [12].

II. PHYSICS OF OTT+11 (O11) COLLAPSAR WAVEFORMS

There are three (3) primary phases associated with approximate approaches in specifically collapsar simulations. In phase 1, GR simulations implement neutrino cooling in which the dynamics after BH formation to the formation of accretion disk is followed. Phase 2 is primarily concerned with the subsequent evolution of the accretion disk and the outflow formation in the polar funnel region until the jets become mildly relativistic. And, phase 3 is mainly concerned with the dynamics from the jet propagation to the breakout from the star by assuming a manual energy input to the polar funnel region.

Ott et al. (2011) [1] extracted the GW signals based on their collapsar simulations (in phase 1). Based on their three-dimensional GR simulations of a 75 $M_\odot$ star using a polytropic EoS, they pointed out that the significant GW emission is associated with the moment of BH formation. A number of semi-analytical estimates have been reported so far that predict a significantly strong GW emission due to possible density inhomogeneities, bar or fragmentation instabilities in the collapsar's accretion torii, and the precession of the disks due to GR effects.

The collapsar waveform, u75, was derived from Ott et al. 2011 [1], where the models possessed time, given in milliseconds, and h_+D, the plus polarization given in units of centimeters (where D is the distance to the source), and had possessed a realistic progenitor, rotation based on the results of stellar evolution calculations, and a simplified equation of state (EoS). The waveform itself possess collapse, bounce, the post-bounce phase, black hole formation, and following the hyper-accretion phase.

u75 is a 75 $M_\odot$, 10^{-4} [1] solar metallicity model whose compact core favors early BH formation. The three models considered are u75rota, u75rotb, and u75rotc, which are given initial angular velocities of 1, 1.5, and 2 rad s^{-1}, respectively. The viability of u75 depends on the GRB progenitor and if the mass transfer to a binary companion has removed H/He envelopes. Overall, the introduction of a more realistic, stiffer EoS will increase the delay between bounce and BH formation, which will then lead to higher amplitude, lower-frequency GWs. The waveforms were specified a sampling frequency of $f_s = 8192$ Hz for the strain.

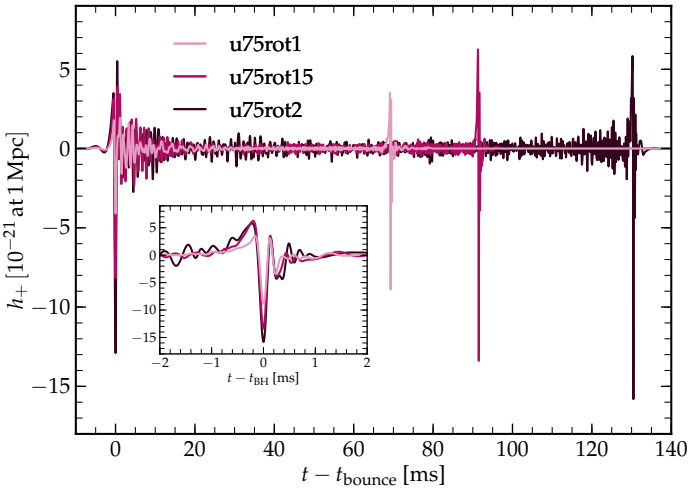

FIG. 1: GW signals, h_+, emitted by the rotating collapsar models as seen by an equatorial observer and rescaled by distance D [1].

III. SEARCH METHODOLOGY REGARDING THE OTT+11 (O11) COLLAPSAR WAVEFORM

A. Coherent Waveburst Pipeline (cWB)

The cWB analysis is based on computing a constrained likelihood function, where each detector data stream is broken down into 6 different wavelet decompositions, each with different time and frequency resolutions. The data are then whitened, and the largest 0.1% of wavelet magnitudes belonging to each frequency bin and interferometer decomposition are retained (hereby known as black pixels). Halo pixels are also retained as they surround the identified black pixels. The selection of pixels that are more likely related to a GW candidate event, clusters of them are identified. Once all wavelet decompositions are projected onto the same time-frequency plane, the clusters are then defined as sets of contiguous retained black or halo pixels. For each cluster of wavelets, a Gaussian likelihood function is computed where the unknown GW is reconstructed with a maximum-likelihood estimator. The likelihood analysis is then repeated over a targeted grid of sky positions covering the range of possible directions to the potential GW source.

Running the waveform through the Coherent Waveburst Pipeline (cWB), which does not require detailed

assumptions about the GW morphology and looks for GW transients in the 60 - 2000 Hz frequency band, the collapsar waveform was injected at specific distances every 100 s plus a randomly selected time varying in the [-10, 10] s band into the time-shifted background data.

B. Distance Estimates for O11 Collapsar Waveform with cWB

Given the loudest event, the detection efficiency as a function of distance for the search is computed. The detection efficiency, in short, is the measurement of the fraction of simulated signals that produce events which survive the coherent tests and data quality cuts and possess a false alarm rate (FAR) lower than the loudest event. For the detection efficiency for phenomenological waveforms, since these waveforms have no intrinsic distance scale, the efficiency is measured as a function of the root-sum square amplitude, h_{rss}. The half-maximum efficiency is used instead of the 50% efficiency as the maximum efficiency is limited by the fraction of the on-source window that is defined by the coverage by coincident data. Therefore, through the usage of the half-maximum, we achieve a measure of the distance reach of the instruments independent of their duty cycles. This was repeated for a range of distances in order to determine a detection efficiency as a function of distance.

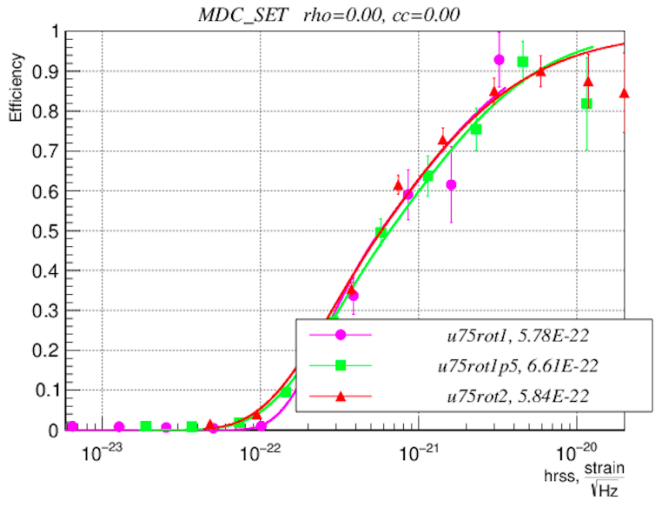

FIG. 2: Detection Efficiency plot for the O11 Collapsar Waveform rescaled to 10 kpc.

IV. PHYSICS OF THE PIRO & THRANE 12 (PT12) WAVEFORMS

GWs from neutron stars that are being spun up by fallback accretion. It is expected that during a CCSNe, a neutron star is born first within the mass ranges from 25 - 40 $M_\odot$, which will usually collapse to a black hole from fallback accretion. Keeping the radius, R, fixed as the mass, M, changes, which is consistent with most EoS, except when M is near its maximum value. When $\beta = \beta_{crit}$, then instabilities rise that then produce GWs [2].

By starting to parameterize the fallback accretion rate to understand the results of MacFadyen et al (2001) and Zhang et al. (2008). This is approximated by two power laws. At early times, the accretion rate scales as

$$\dot{M}_{\rm early} = \eta 10^{-3} t^{1/2} M_\odot s^{-1} \tag{1}$$

where $\eta = 0.1 - 10$, which is a factor that accounts for different explosion energies, and t is measured in seconds. The late time accretion is independent of the explosion energy and is set to be the following

$$\dot{M}_{\rm late} = 50 t^{-5/3} M_\odot s^{-1} \tag{2}$$

And, the accretion rate at any given time is found from interpolating the two expressions above.

$$\dot{M} = (\dot{M}^{-1}_{early} + \dot{M}^{-1}_{late}) \tag{3}$$

The neutron star has $M_0 = 1.3\ M_\odot$ and R = 20 km, and $\eta = 1.0$ for setting M. It is assumed that the neutron star accretes for 100 sec during which $\beta \leq \beta_{crit}$ and no angular momentum is lost. We then set $\beta = \beta_{crit} = 0.14$ and follow the [evolution up until M = 2.5 $M_\odot$, at which point the neutron star would collapse to become a black hole.

The estimation of actual waveforms depends on two equations that are representative for the two polarizations, h_+ and h_x.

$$h_+(t) = h_0(1 + \cos^2 i)\cos(2\pi {\rm ft}) \tag{4}$$

$$h_{\rm x}(t) = 2h_0 \cos i \sin(2\pi {\rm ft}) \tag{5}$$

where $f = \Omega/\pi$ is the gravitational wave frequency and i is the inclination of the source. The characteristic amplitude measured by gravitational wave detectors is $h_{\rm c} = f h_0 \sqrt{dt/df}$, where $\rm h_0$ is defined as being the following.

$$\rm h_0 = \frac{2G}{c^4}\frac{Q\Omega^2}{D} \tag{6}$$

where D is the distance to the source, Q is the quadrupole moment, and Ω^2 is the spin of the neutron star.

O11 Optimal SNR at 1 Mpc						
Waveforms	aLIGO	AdVirgo	KAGRA	Voyager	Einstein Telescope	Cosmic Explorer
u75a	0.4	0.2	0.2	1.1	3.8	6.2
u75b	0.7	0.4	0.4	2.1	7.2	11.7
u75c	0.9	0.5	0.5	3	9.9	16.2

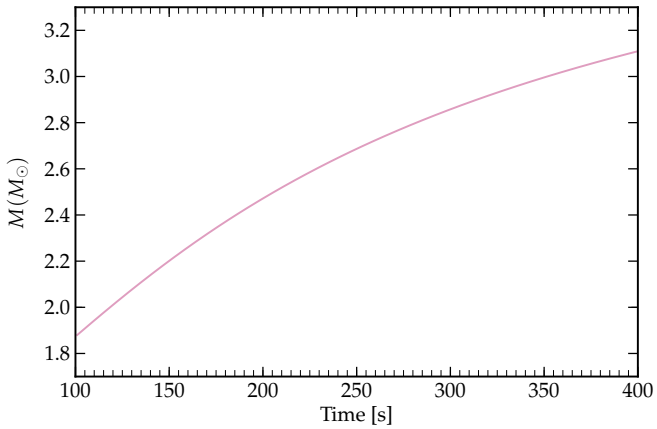

FIG. 3: Example mass evolution, with the neutron star possessing an initial mass, $M_0 = 1.3\ M_\odot$, with a radius, R = 20 km.

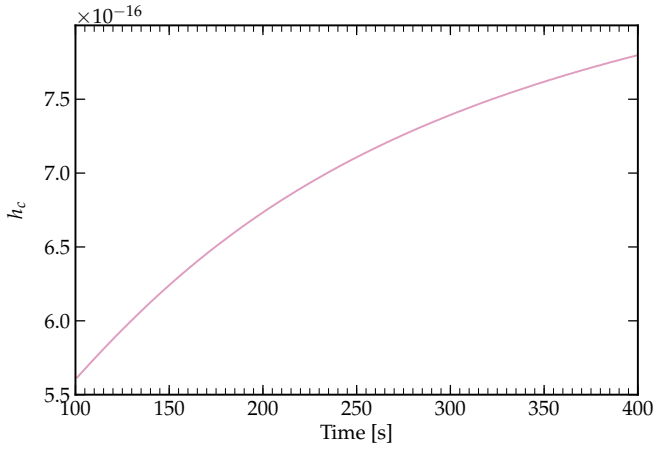

FIG. 4: An example strain amplitude evolution, where the corresponding strain from these GWs is as measured on Earth, where D is the distance to the source.

TABLE I: PT12 Model Parameters

Initial Mass of NS	$M_0 = 1.3\ \mathrm{M}_\odot$
Constant NS Radius	R = 20 km
Explosion Energy	$\eta = [0.1, 10]$
$\beta > \beta_c$	$\mathrm{t}_{\mathrm{initial}}$
GW emission stops	$\mathrm{t}_{\mathrm{final}}$

V. PARAMETERIZING THE NEUTRON STAR EQUATION OF STATE

As stars approach their final stages of plunge and merger, the GW phase accumulates more rapidly for smaller values of the ratio of the mass of the neutron star to its radius. In order to systematize the study of constraints placed by astrophysical observations on the nature of neutron-star matter and GW emission, we estimate that a realistic equation of state (EoS) will lead to gravitational waveforms that are distinguishable at an effective distance to an optimally oriented and located system that would produce an equivalent waveform amplitude of 20 Mpc or less.

The most recent constraint regarding the mass-radius relation of NS are provided from data taken of pulsars by the values of the largest mass, the largest radius, the highest rotational frequency, and the maximum surface gravity. Until now, the largest NS mass measured is the mass of the 39.12 ms pulsar PSR J0348+0432, $\mathrm{M} = 2.01 \pm 0.04\mathrm{M}_\odot$ [13]. The largest radius is given by the lower limit to the radius of RX J1856-3754, as seen by an observer at infinity, $\mathrm{R}_\infty = \mathrm{R}[1 - 2\mathrm{GM}/(\mathrm{c}^2\mathrm{R})]^{-1/2} \geq$ 16.8km,[14]. The maximum surface gravity is obtained by assuming a NS of $\mathrm{M} = 1.4\mathrm{M}_\odot$ in order to fit the Chandra data of the low-mass X-ray binary X7. The maximum rotation rate of a neutron star has been found to be $\mathrm{v}_{\mathrm{max}} = 1045(\mathrm{M}/\mathrm{M}_\odot)^{1/2}(10\mathrm{km}/\mathrm{R})^{3/2}$ Hz [14]. The fastest observed pulsar is PSR J1748-2246ad with a rotational frequency of 716 Hz,[14], which results in the constraint $\mathrm{M} \geq 0.47(\mathrm{R}/10\mathrm{km})^3\mathrm{M}_\odot$.

We reference the table provided in O'Connor & Ott (2010) by matching the high densities of the EoS of Lattimer & Swesty (1991), which possesses a nuclear compressibility of $K = 220\,\mathrm{MeV}$, with densities below $10^8\,\mathrm{g\,cm^{-3}}$ referencing to the EoS of Timmes & Arnett (1999). Understanding that we are targeting GW emission from massive, rapidly-rotating astrophysical objects with sub-solar metallicity that may very likely fail to produce a SN explosion, we constrain an initial model where the maximum baryonic mass supported will be 2.41 $M_\odot$. The formation of a BH in a stellar core-collapse will not realistically occur of the iron core, but will extend, generally, to timescales longer that 0.5 s [15]. In the collapsar scenario, a lower limit may be estimated at times where 2.41 $M_\odot$ have been accreted through the shock around 820 ms and the maximum mass has the possibility of being modified by the effects of rotation and temperature. Introducing a stiffer EoS would allow for larger maximum masses and therefore longer associated collapse times.

Variations of the P12 Collapsar Waveform						
Waveforms	Radius (km)	η	M_{max}	$t_{initial}$ (s)	t_{final} (s)	Duration
PT12a	12	0.1	2	489.5	748.3	258.8
PT12b	12	1	2	89.3	118.3	29.3
PT12c	12	5	2	29.3	37.7	8.4
PT12d	14.5	0.1	2.2	480.9	1176.9	696
PT12e	14.5	1	2.2	88.2	149.6	61.4
PT12f	14.5	5	2.2	28.9	45.9	17

PT12 h_{rss} at 1 Mpc	
Waveforms	h_{rss}
PT12a	3.6540×10^{-22}
PT12b	3.6547×10^{-22}
PT12c	3.6556×10^{-22}
PT12d	6.4001×10^{-22}
PT12e	6.4010×10^{-22}
PT12f	6.4020×10^{-22}

VI. GILL & GOSSAN 2016 (GG16) PHENOMENOLOGICAL WAVEFORM

It is important to emphasize that the phenomenological collapsar waveform, although astrophysically improved, should be considered as being at the extreme end of plausible GW emission scenarios at relatively near distances within 20 Mpc. Taking the analysis of the PT12 waveform, we improved the previous collapsar models by introducing more astrophysically realistic parameters. Aspects that were improved on included the following:

- Introduced parameterization of the accretion rate if the shape of the spun up neutron star slowly becomes bar-like over time.
- Took into account the internal circulation patterns that are caused by secular instabilities, which produce significant GW power at lower frequencies, and therefore matched the analytical model better to current detector, such as aLIGO, and future detector noise curves.
- Introduced a range of values for the quadrupole moment that will be sufficient to balance the accretion torques that exceed the maximum strain the neutron star crust is able to support.
- Understanding on how external material behaves as it accumulates on the top of the neutron star as the core becomes more compressed and redid PT12 analytical templates. Overall, an analysis was conducted on how the β and mass/radius relationship evolves over time.

In order to understand the evolution of the beta, mass/radius, and strain relationship over time, there was an implementation of a realistic EoS. The radius was derived from the mass evolution through the introduction of 7 finite temperature EoS. The evolution of β was set to $t = t_{initial}$ when $\beta = \beta_c$. The evolution of mass was set to $t = t_{final}$ when $M > M_{max}$.

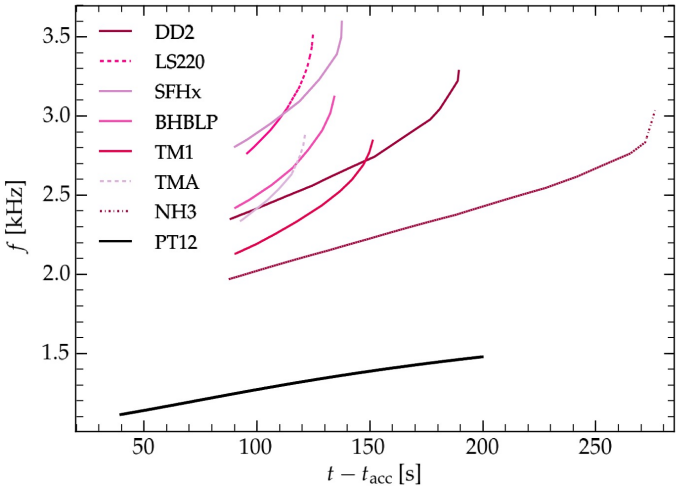

FIG. 5: GG16 frequency evolution, with the neutron star possessing an initial mass, $M_0 = 1.3\ M_\odot$, for 7 finite-temperature EoS.

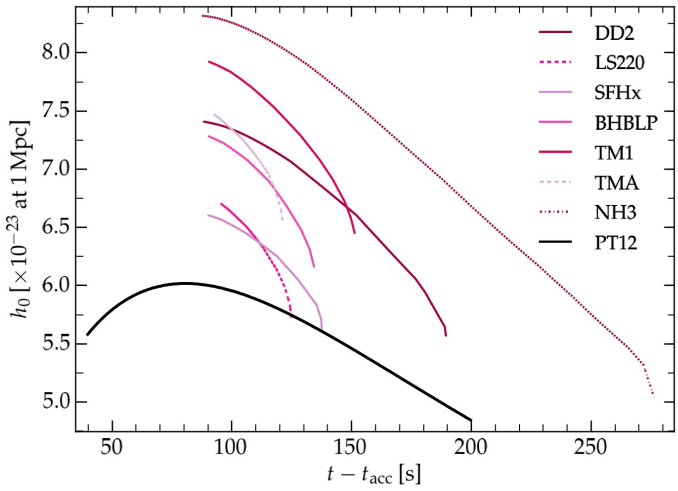

FIG. 6: GG16 strain evolution, with the neutron star possessing an initial mass, $M_0 = 1.3\ M_\odot$, for 7 finite-temperature EoS. The strain although larger, is at higher frequencies due to the fact the waveform model stops when GW emission is achieved through both initial core-collapse and subsequent BH formation and ringdown.

TABLE II: PT12/GG16 Model Comparison

$M_0 = 1.3$ M$_\odot$	$M_0 = 1.3$ M$_\odot$
R = 20 km	R(M) from 7 finite-temp EoS
$\beta_c = 0.14$	$\beta_c = 0.14$
η = [0.1, 10]	$\eta = 1$
$t_{\rm initial,PT12} = 40$ s	$t_{\rm initial,GG16}$ from $\beta > \beta_c$
$t_{\rm final,PT12} = 200$ s	$t_{\rm final,GG16}$ from M > M$_{\rm max}$

VII. THE CONNECTION BETWEEN LONG GAMMA-RAY BURSTS (LGRBS) AND TYPE IC-BL SNE

The collapsar scenario involves a rotating massive star whose core collapses to a black hole (BH) and produces an accretion disk. The collapsar progenitors typically have two requirements needed to be satisfied: the core collapse produces a BH either promptly/shortly thereafter and there must be sufficient angular momentum that exists in order to form a disk outside the BH. In the collapsar scenario [15, 16], the high rotation required to form the centrifugally supported disk should produce gravitational waves (GWs) via bar [17–20] or fragmentation instabilities that potentially develops within the collapsing core [21] and/or in the disk [22–24]. Furthermore, the collapsar scenario is observationally supported by the fact that long gamma-ray bursts (LGRBs) occur in galaxies with high specific star formation rate [25, 26]. More specifically, the association of LGRBs with star forming regions, and in several cases with type Ic-BL SNe, suggest that they involve stellar collapse.

Broad-line type Ic SNe (Ic-BL) are a type of highly energetic supernovae that are associated with LGRBs. The population of LGRB-SNe isn't correlated with subset of type Ic SNe, as specifically broad-line type Ic SNe follow the metallically distribution of star-formation in a general galaxy population [27]. It is worth noting that LGRB associated events do posses unusually broad spectral features [28].

The concentration of kinetic energy in relativistic ejecta ($\beta\Gamma \geq 2$) is the distinguishing feature of a GRB-SN. Here, β is the velocity of the ejecta divided by the speed of light and the Lorentz factor $\Gamma = (1-\beta^2)^{-1/2}$. The value of the energy of the gamma-rays, E_γ, is difficult to measure directly because of the effects of beaming, but in typical bursts, it is around 10^{51} erg. The energy in relativistic ejecta,$E_{\rm Rel}$, may be inferred from radio observations at such late times that beaming is no longer important, and is 5×10^{51} erg.

Understanding that a fraction of LGRBs are missed due to their beaming angles being unaligned toward the direction of the Earth, we only consider the LGRBs aligned in the direction of the Earth. Therefore, a beaming fraction is defined according to the burst's beaming angle, which depends on the uniform beam or structured beam (i.e. where the Lorentz factor varies with angle). There are two widely different, yet accepted, values of $520^\circ \pm 85^\circ$ and $75^\circ \pm 25^\circ$ [29, 30]. The primary difference between the two angle calculations is that one method assumes the existence of a large number of low-luminosity bursts that cannot be observed except at the closest redshifts, but other methodology [31] has a consistency between the beaming angle population and that of the *Swift* population. But, this methodology also makes certain simplifications in their the jet structure of the LGRBs and assumes any optical break to be a jet break, which is now known to be classified as a poor approximation. To properly constrain and define the jet angle, one of the parameters that is required is the GRB isotropic-equivalent energy release, $E_{\rm iso}$. This requires the burst redshift to be known, but is not available for most LGRBs. Even when $E_{\rm iso}$ is known, the range in opening angles is fairly broad, and therefore the sample sizes are still insufficient enough to determine a distribution, much less a mean angle.

VIII. LOCAL RATE OF BROAD-LINE TYPE IC SNE AND LGRBS

The fraction of type Ic SNe that are broad-line derived from the local core-collapse SNe rate is 0.21 ± 0.05 [32]. The local rate of aligned LGRBs is $0.42^{+0.9}_{-0.4}$ [33]. Knowing these statistics, then assuming a semi-nominal beaming factor of 100, this would lead to approximately 1 out of 40 low metallicity type Ic-BL SNe events that have a potential of giving rise to a LGRB. These results are consistent, given the absence of off-axis LGRB detections in radio surveys of broad-line type Ic-BL SNe events. Given the 1 out of 40 rate estimated, a minimal sample size of a hundred low metallicity SNe would be required in order to be reasonably confident of detecting an off-axis LGRB. It's important to note that a search performed for LGRBs without any regard to galaxy metallicity would be 5 times less effective in finding a LGRB. A proposal of a radio search that takes into account the low metallicity optimized off-axis LGRB would lead to at least a 90% detection efficiency of off-axis LGRBs.

IX. PROPOSED RADIO SEARCH

Merger events with gamma-rays beamed away from Earth, essentially denoted as off-axis gamma-rays, would

be invisible to gamma-ray surveys conducted by satellites, such as *Swift* [34]. But, GWs and the resulting afterglow radiation would be emitted and present a wider possibility of detection. Proposed searches, such as a GW triggered search, could potentially aid in the detection of orphan afterglows associated with off-axis events. Early observations have led the understanding that short-hard bursts possess beaming fractions of one to a few percent, or opening angles of roughly 10 degrees. This suggests that off-axis events are far more common than on-axis events, therefore pointing to the conclusion that the rate of orphan afterglows may be significantly greater than the rate of observable GRBs. An appealing prospect is presented by the possibility of using GWs to trigger EM (radio, optical, X-ray, gamma) follow-ups of GW sources [35–37]. The discovery of an off-axis optical or radio afterglow, which would be triggered from the non-beamed GW emission from the GRB progenitor, would led to the confirmation of the jet model, map out the beaming distribution of the GRB itself, as well as providing the fundamental understanding to the models of relativistic outflows.

We propose a radio search focusing entirely on type Ic-BL SNe in low metallicity environments, defined as $\log[\mathrm{O/H}] + 12 \leq 8.4$, containing roughly 90 targets in order to determine at least a 90% chance of detecting an off-axis LGRB event. The realistic problem we are faced with is finding roughly 100 type Ic-BL SNe within low metallicity environments that simultaneously contain 10% of star formation activity and are close enough in order to permit successful radio observations. If recent advances in nearby CCSNe search capabilities (i.e. ZTF) provide the capability to find at least 50% of the predicted events, then there is a real possibility of finding an off-axis LGRB within the next decade and constraining an upper limit rate on the expected number of LGRBs found in association with type Ic-BL SNe within the local universe. For example, the Zwicky Transient Facility

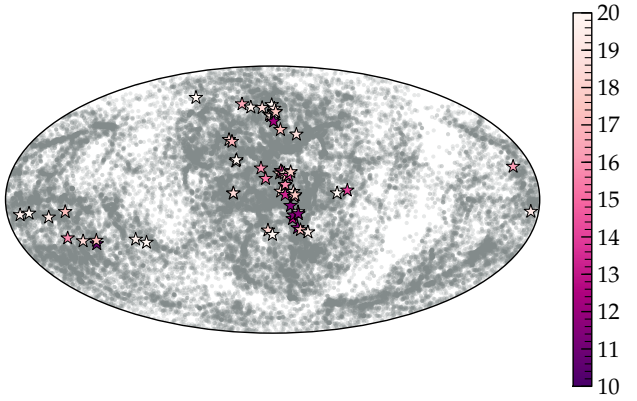

FIG. 7: Identified starburst clusters within 20 Mpc that serve as potential survey targets for the detection of LGRB emission and type Ic SNe.

(ZTF) [38] is the next-generation optical synoptic survey that will provide the best characterization of the bright to moderate-depth transient and variable sky. And, with ZTF's wider, fast camera, the collaboration will be able to study a true sample of SN progenitors and will be able to detect one Sn within 24 hours of its explosion every night. The fraction of radio SNe Ic, where the peak emission is at 5 GHz in less than 10 days, is not well constrained. A possible strategy is to better study the rapidly evolving radio SN by conducting observations at lower frequencies, such as 1.4 GHz. Another appealing potential search is represented by the possibility of using GWs to trigger EM follow-ups of GW searches.

X. CONCLUSION

We investigated the production of GWs resulting from a subset of SNe where a NS is produced within the core, but subsequently collapses to a BH after roughly 30 - 3000 s of fallback accretion. Introducing a phenomenological waveform model for the mass/radius evolution of the NS over a period of time until GW emission occurs, corresponding to frequencies within 500 - 4096 kHz.

In order to selectively choose among the existing, accepted models of NS, the current observational constraints on the mass-radius relations related to the maximum observed mass, maximum surface gravity, largest mass, and maximum rotation frequency have been analyzed. All these constraints are of paramount importance in not only in the physics of neutron stars, but also to correctly test and further astrophysically constrain assumptions made in the constructions of the EoS. This initial work involves multiple astrophysical improvements in the GW model including: using realistic fallback rates from numerical models, understand how the external material on the top of the spinning neutron star behaves as the core becomes compressed by introducing the evolution of β, mass/radius, and strain relationship over time through the implementation of 7 finite temperature EoS, as well as determining range of frequencies at the moment before collapse to a BH that directly constrained the density at the maximum mass of a NS.

A radio search was proposed focusing on increasing the number of observed detections of type Ic-BL SNe within 20 Mpc in low metallicity environments in order to determine a 90% chance of detecting an off-axis LGRB event and essentially increasing the possibility of detecting GW emission from the collapsar mechanism in the context of Advanced LIGO, Advanced Virgo, and future third-generation ground-based GW detectors.

XI. ACKNOWLEDGEMENTS

We thank Anthony Piro for detailed discussions on the physics behind the evolution of the mass/radius relationship and on the hotly debating topic concerning constraining the neutron star equation of state. We also

thank Mansi Kasliwal and Joeri van Leeuwen for insight into the radio survey proposal process within the astronomy community and for evaluating the feasibility of our proposed radio search tailored for increased observational type Ic-BL SNe discoveries within the range of the advanced generation detector network. We thank the support of both NSF and the Caltech LIGO-SURF program.

[1] C. D. Ott, C. Reisswig, E. Schnetter, E. O'Connor, U. Sperhake, F. Löffler, P. Diener, E. Abdikamalov, I. Hawke, and A. Burrows, Physical Review Letters **106**, 161103 (2011), 1012.1853.

[2] A. L. Piro and E. Thrane, Astrophys. J. **761**, 63 (2012), 1207.3805.

[3] C. S. Kochanek, J. F. Beacom, M. D. Kistler, J. L. Prieto, K. Z. Stanek, T. A. Thompson, and H. Yüksel, Astrophys. J. **684**, 1336-1342 (2008), 0802.0456.

[4] C. L. Fryer, P. A. Mazzali, J. Prochaska, E. Cappellaro, A. Panaitescu, E. Berger, M. van Putten, E. P. J. van den Heuvel, P. Young, A. Hungerford, et al., Publ. Astron. Soc. Pac. **119**, 1211 (2007), astro-ph/0702338.

[5] C. L. Fryer, P. J. Brown, F. Bufano, J. A. Dahl, C. J. Fontes, L. H. Frey, S. T. Holland, A. L. Hungerford, S. Immler, P. Mazzali, et al., Astrophys. J. **707**, 193 (2009), 0908.0701.

[6] T. Moriya, N. Tominaga, M. Tanaka, K. Nomoto, D. N. Sauer, P. A. Mazzali, K. Maeda, and T. Suzuki, Astrophys. J. **719**, 1445 (2010), 1006.5336.

[7] X. Y. Wang, Z. G. Dai, T. Lu, D. M. Wei, and Y. F. Huang, Astron. Astrophys. **357**, 543 (2000), astro-ph/9910029.

[8] J. Hjorth, Philosophical Transactions of the Royal Society of London Series A **371**, 20120275 (2013), 1304.7736.

[9] S. Akiyama and J. C. Wheeler, Astrophys. J. **629**, 414 (2005), astro-ph/0504563.

[10] A. I. MacFadyen and S. E. Woosley, Astrophys. J. **524**, 262 (1999), astro-ph/9810274.

[11] K. W. Weiler, S. D. van Dyk, R. A. Sramek, N. Panagia, C. J. Stockdale, and M. J. Montes, in *1604-2004: Supernovae as Cosmological Lighthouses*, edited by M. Turatto, S. Benetti, L. Zampieri, and W. Shea (2005), vol. 342 of *Astronomical Society of the Pacific Conference Series*, p. 290.

[12] O. L. Caballero, T. Zielinski, G. C. McLaughlin, and R. Surman, Phys. Rev. D. **93**, 123015 (2016), 1510.06011.

[13] J. Antoniadis, P. C. C. Freire, N. Wex, T. M. Tauris, R. S. Lynch, M. H. van Kerkwijk, M. Kramer, C. Bassa, V. S. Dhillon, T. Driebe, et al., Science **340**, 448 (2013), 1304.6875.

[14] J. M. Lattimer and M. Prakash, Science **304**, 536 (2004), astro-ph/0405262.

[15] S. E. Woosley and A. I. MacFadyen, Astron. Astrophys. Suppl. **138**, 499 (1999).

[16] B. Paczyński, Astrophys. J. Lett. **494**, L45 (1998), astro-ph/9710086.

[17] J. L. Houser, J. M. Centrella, and S. C. Smith, Physical Review Letters **72**, 1314 (1994), gr-qc/9409057.

[18] K. C. B. New, J. M. Centrella, and J. E. Tohline, Phys. Rev. D. **62**, 064019 (2000), astro-ph/9911525.

[19] L. Baiotti, I. Hawke, and L. Rezzolla, Classical and Quantum Gravity **24**, S187 (2007), gr-qc/0701043.

[20] H. Dimmelmeier, C. D. Ott, A. Marek, and H.-T. Janka, Phys. Rev. D. **78**, 064056 (2008), 0806.4953.

[21] C. Ott, *Predicting the electromagnetic, gravitational wave, and neutrino signature of short gamma-ray burst central engines with general-relativistic neutrino-radiation-MHD simulations of the merger of double neutron star and neutron-star–black-hole binaries.*, NASA ATP Proposal (2010).

[22] C. L. Fryer, D. E. Holz, S. A. Hughes, and M. S. Warren, ArXiv Astrophysics e-prints (2002), astro-ph/0211609.

[23] S. Kobayashi and P. Mészáros, in *The Astrophysics of Gravitational Wave Sources*, edited by J. M. Centrella (2003), vol. 686 of *American Institute of Physics Conference Series*, pp. 84–87.

[24] A. L. Piro and E. Pfahl, Astrophys. J. **658**, 1173 (2007), astro-ph/0610696.

[25] A. S. Fruchter, A. J. Levan, L. Strolger, P. M. Vreeswijk, S. E. Thorsett, D. Bersier, I. Burud, J. M. Castro Cerón, A. J. Castro-Tirado, C. Conselice, et al., Nature **441**, 463 (2006), astro-ph/0603537.

[26] E. M. Levesque, L. J. Kewley, E. Berger, and H. J. Zahid, Astron. J. **140**, 1557 (2010), 1006.3560.

[27] J. F. Graham and A. S. Fruchter, Astrophys. J. **774**, 119 (2013), 1211.7068.

[28] M. Modjaz, R. P. Kirshner, S. Blondin, P. Challis, and T. Matheson, Astrophys. J. Lett. **687**, L9 (2008), 0801.0221.

[29] D. A. Frail, S. R. Kulkarni, R. Sari, S. G. Djorgovski, J. S. Bloom, T. J. Galama, D. E. Reichart, E. Berger, F. A. Harrison, P. A. Price, et al., Astrophys. J. Lett. **562**, L55 (2001), astro-ph/0102282.

[30] D. Guetta, T. Piran, and E. Waxman, Astrophys. J. **619**, 412 (2005), astro-ph/0311488.

[31] H.-Y. Chen and D. E. Holz, Physical Review Letters **111**, 181101 (2013), 1206.0703.

[32] P. L. Kelly and R. P. Kirshner, Astrophys. J. **759**, 107 (2012), 1110.1377.

[33] A. Lien, T. Sakamoto, N. Gehrels, D. M. Palmer, S. D. Barthelmy, C. Graziani, and J. K. Cannizzo, Astrophys. J. **783**, 24 (2014), 1311.4567.

[34] M. Nardini, G. Ghisellini, G. Ghirlanda, and A. Celotti, Mon. Not. R. Astron. Soc. **403**, 1131 (2010), 0907.4157.

[35] J. Sylvestre, Astrophys. J. **591**, 1152 (2003), astro-ph/0303512.

[36] B. Cobb, C. Bailyn, and J. Bloom, *Optical/IR Follow-Up of Gamma-Ray Bursts from SMARTS*, NOAO Proposal (2009).

[37] B. D. Metzger and E. Berger, Astrophys. J. **746**, 48 (2012), 1108.6056.

[38] S. R. Kulkarni, in *American Astronomical Society Meeting Abstracts* (2016), vol. 227 of *American Astronomical Society Meeting Abstracts*, p. 314.01.